

## Study of the composition around the knee through the electromagnetic and muon detectors data at EAS-TOP

B. Alessandro for THE EAS-TOP COLLABORATION

I.N.F.N. Torino, Italy

**Abstract.** The cosmic ray primary composition is studied around the knee ( $E_0 \simeq 3 \cdot 10^{15}$  eV) of the primary energy spectrum with the EAS-TOP array. The fluctuations in the number of muons recorded at  $\approx 200$  m from the core in narrow intervals of shower sizes are compared with the expectations obtained from simulations performed with the CORSIKA/QGSJET code. From the analysis of vertical showers an increase in the average primary mass in the energy range  $E_0 = 2 \cdot 10^{15} - 8 \cdot 10^{15}$  eV is deduced. A preliminary analysis in more inclined directions is consistent with such result.

### 1 Introduction

The study of the relation between the electron and muon numbers in Extensive Air Showers (EAS), their fluctuations and relative variations still represent one of the main techniques to obtain information on the cosmic ray primary composition at energies above  $10^{15}$  eV, and it is therefore a key to the understanding of the physical origin of the knee. Such studies are performed by means of the electromagnetic (e.m.) and GeV muon detectors of EAS-TOP (Aglietta M. et al. 1993) located at Campo Imperatore, National Gran Sasso Laboratories, 2005 m a.s.l.,  $820 \text{ g} \cdot \text{cm}^{-2}$  atmospheric depth.

At previous ICRCs we presented results of the behaviour of the average values of the muon number ( $N_\mu$ ) vs shower size ( $N_e$ ) (Eas-Top Collaboration 1997) and (Chiavassa A. et al. 1999). The anomalous increase of  $N_\mu$  with respect to the expectations from a constant composition supports an increase of the average cosmic ray mass ( $\langle A \rangle$ ) with primary energy in the region of the knee.

In this paper we present an analysis of the fluctuations of the number of muons at fixed core distance ( $N_{\mu 200}$ , measured by the muon-hadron detector), in different narrow intervals of shower size ( $N_e$ , measured by the e.m. array). The experimental data are interpreted by means of simulations based

on the CORSIKA/QGSJET code (Heck D. et al. 1998).

### 2 The detectors and the data

The EAS-TOP e.m. array consists of 35 modules  $10 \text{ m}^2$  each of plastic scintillators distributed over an area of  $10^5 \text{ m}^2$ . In the present work, events with at least six neighboring modules fired, and the largest number of particles recorded by a module internal to the edges of the array ("internal events") are selected. The core location ( $X_c, Y_c$ ), the shower size  $N_e$  and the slope of the lateral distribution function  $s$  are obtained fitting the recorded number of particles in each module with the Nishimura-Kamata-Greisen (NKG) expression (Kamata K. et al. 1958). The resolutions of such measurements have been calculated by analyzing simulated events in which all experimental uncertainties have been included. Comparing generated events with reconstructed ones for shower sizes  $N_e > 2 \cdot 10^5$  where the detection efficiency is  $\epsilon \sim 100\%$  we obtain:  $\sigma_{N_e}/N_e \simeq 0.1$ ;  $\sigma_{X_c} = \sigma_{Y_c} \simeq 5 \text{ m}$ ;  $\sigma_s \simeq 0.1$ .

The shower arrival direction is measured from the times of flight among the different modules. The resolution for internal trigger events is  $\sigma_\theta \simeq 0.9^\circ$

The muon-hadron detector in these measurements is used as a tracking module of 9 active planes. Each plane has two layers of streamer tubes (12 m length,  $3 \times 3 \text{ cm}^2$  section) for muon tracking, one layer of proportional tubes for hadron calorimetry, 8 cm of air and 13 cm of iron shield. The total height of the detector is 280 cm and the surface is  $12 \times 12 \text{ m}^2$ . The X coordinate of the crossing particle is measured from the signals of the anode wires, the Y one from the induced signals on 3 cm width strips located orthogonal to the wires, the Z one from the height of the layer. A muon track is defined from the alignment of at least 6 fired wires in different streamer tube layers. The detection efficiency is 97% up to 10 particles crossing the detector decreasing to 93% for 20 particles. The tracker efficiency becomes significantly worse when more than 40 muons cross the detector. The muon energy threshold is  $E \simeq 1 \text{ GeV}$  for vertical inci-

dence.

A sample of experimental data corresponding to 150 days of data taking has been used.

### 3 The simulation

Events have been simulated with the CORSIKA code using QGSJET as high energy hadronic interaction model and the analytic treatment of the e.m. component given by the NKG formula. The full response of the muon detector is included by means of simulations based on the Geant code, and the measured experimental efficiencies of the streamer tubes. The fluctuations in the number of particles and the transition effects have been included in the response of the e.m. modules through Geant simulations whose results have been parametrized, including all experimental uncertainties. The simulated events for both detectors have been treated in the same way as the experimental data.

The primary spectra are simulated with power spectrum index  $\gamma = 2.75$  for all elements with a factor 3 of oversampling. Due to the narrow intervals of  $N_e$  used in this analysis, small differences in the spectrum steepness do not affect the results. The nuclear elements introduced in the simulations are: p, He, N, Mg, Fe for a number of events almost equal to the experimental ones.

The capability of the CORSIKA/QGSJET code for describing the EAS properties has been extensively studied by the KASCADE group, mainly through the hadrons in EAS in the region around the knee (Kascade Collaboration 1999 a), and through the EAS-TOP hadron and high energy muons plus Cherenkov light data up to about  $10^{14}$  eV (Eas-Top Collaboration 2001).

### 4 Analysis and results

The analysis is performed for vertical showers ( $1 < \text{sec}\theta < 1.05$ ) in the range of size  $5.4 < \text{Log}(N_e) < 6.6$ , i.e. just across the knee ( $\text{Log}(N_e) \simeq 6.13$ ). The parameters used in the analysis are the shower size  $N_e$  and the muon number observed in the muon detector for core distances  $180 < r_c < 210$  m ( $N_{\mu 200}$ ). Such variable  $N_{\mu 200}$  reduces the statistics, but such loss is compensated by the advantage of working in a narrow range of core distances, so that no use of the muon l.d.f. is required.

As a first information, the observed average  $N_{\mu 200}$  vs  $N_e$  relation is compared in fig. 1 with the expectations from the single components. The same plot is given in fig. 2 for more inclined events ( $1.1 < \text{sec}\theta < 1.15$ ). The results are consistent, showing that the experimental data drift, with increasing shower size, from the helium to the N (for CNO) simulated data. The lower point in both cases is in very good agreement with the expectations from an extrapolated low energy composition (Chiavassa A. et al. 1999).

The evolution of the abundances of the individual components has been studied by fitting the experimental  $N_{\mu 200}$  dis-

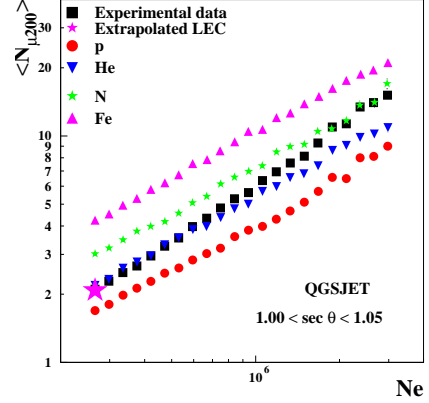


**Fig. 1.**  $\langle N_{\mu 200} \rangle$  vs  $N_e$  relation in experimental data for vertical showers together with the expectations from single elements; the big star shows the expectation from the extrapolated low energy composition.

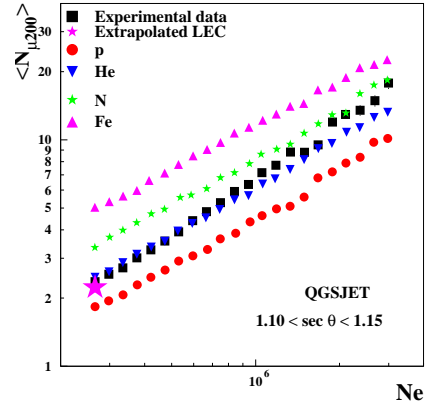


**Fig. 2.** Same as fig. 1 for inclined showers ( $1.10 < \text{sec}\theta < 1.15$ ).

tributions measured in ranges of shower sizes ( $\Delta \text{Log}(N_e) = 0.2$ ) with the simulated ones, optimizing the relative weights.

As a first step it has been verified that single components cannot fit the experimental  $N_{\mu 200}$  distributions. In table 1, for each element, the  $\chi^2$  values obtained after normalization of the experimental and calculated distributions are given for the six intervals of  $\text{Log}(N_e)$ .

The large  $\chi^2$  values and the inadequacy in the description of the tails of the distributions (see fig. 3, for N primaries, in the bin corresponding to the knee) clearly indicate the impossibility to explain the experimental distributions with a single element in the bins of shower size with sufficient statistics.

As a second step the data have been fitted with a two component composition: a first one ('light') as a mixture 50% proton and 50% helium and a second one ('heavy') represented by iron. The introduction of the 'light' component instead of proton and helium is due at the insensitivity in distinguish them from the experimental point of view, while a 50% abundance of each element seems reasonable at these

$\text{Log}(N_e)$	5.4-5.6	5.6-5.8	5.8-6.0	6.0-6.2	6.2-6.4	6.4-6.6
$p \chi^2$	78.8	46.9	61.7	25.3	11.3	5.0
$He \chi^2$	20.5	8.7	9.2	5.5	4.5	2.8
$N \chi^2$	104.4	37.4	17.9	8.6	2.9	1.0
$Fe \chi^2$	567.3	389.8	146.1	46.9	24.4	6.8
$p + He \chi^2$	26.1	17.2	16.8	9.2	7.2	4.64

**Table 1.**  $\chi^2$  values obtained by fitting the  $N_{\mu 200}$  experimental distributions with a single component each time :  $p$ ,  $N$ ,  $Fe$  and  $p + He$  in different ranges of shower sizes.

$\text{Log}(N_e)$	5.4-5.6	5.6-5.8	5.8-6.0	6.0-6.2	6.2-6.4	6.4-6.6
$p+He$	$0.87 \pm 0.03$	$0.87 \pm 0.05$	$0.85 \pm 0.06$	$0.84 \pm 0.08$	$0.7 \pm 0.1$	$0.7 \pm 0.1$
$Fe$	$0.13 \pm 0.02$	$0.15 \pm 0.03$	$0.20 \pm 0.03$	$0.23 \pm 0.04$	$0.40 \pm 0.08$	$0.7 \pm 0.1$
$\chi^2$	3.5	4.1	3.0	2.0	2.0	1.5

**Table 2.** Relative abundances of two primary mass components :  $p + He$ ,  $Fe$  in different ranges of shower sizes and relative  $\chi^2$  values obtained by fitting the  $N_{\mu 200}$  experimental distribution. No condition of weight normalization is imposed in the fit.

$\text{Log}(N_e)$	5.4-5.6	5.6-5.8	5.8-6.0	6.0-6.2	6.2-6.4	6.4-6.6
$p+He$	$0.80 \pm 0.05$	$0.73 \pm 0.06$	$0.61 \pm 0.06$	$0.56 \pm 0.05$	$0.38 \pm 0.04$	$0.25 \pm 0.05$
$N$	$0.12 \pm 0.06$	$0.20 \pm 0.07$	$0.30 \pm 0.07$	$0.35 \pm 0.06$	$0.49 \pm 0.06$	$0.61 \pm 0.08$
$Fe$	$0.09 \pm 0.03$	$0.09 \pm 0.03$	$0.11 \pm 0.03$	$0.11 \pm 0.02$	$0.16 \pm 0.03$	$0.23 \pm 0.04$
$\chi^2$	3.0	3.3	1.8	0.9	0.6	0.5

**Table 3.** Relative abundances of three primary mass components :  $p + He$ ,  $N$  and  $Fe$  in different ranges of shower sizes and relative  $\chi^2$  values obtained by fitting the  $N_{\mu 200}$  experimental distribution

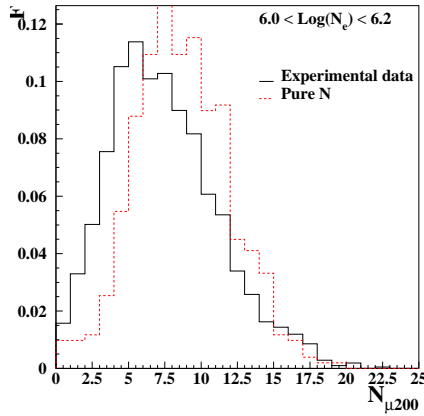


**Fig. 3.**  $N_{\mu 200}$  distribution of the data compared with the expectation from a single component ( $N$ ). The total experimental number of events is  $N_t = 2294$ .

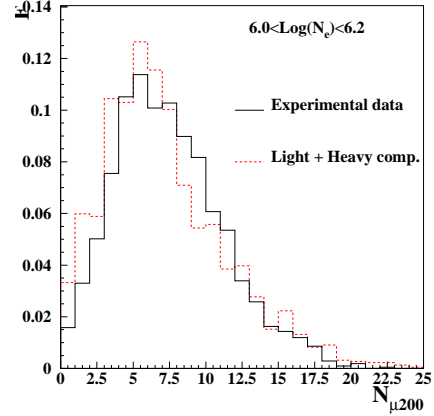


**Fig. 4.**  $N_{\mu 200}$  distribution of the experimental data together with the expectation from a two component composition ('light' and 'heavy'). ( $N_t = 2294$ ).

energies, for the present accuracies. The obtained relative abundances of 'light' and 'heavy' elements in each range of  $N_e$  and the  $\chi^2$  values are given in table 2. The values of  $\chi^2$  still indicate that the experimental distribution is not fully described by such two component model (a typical distribution, for the same size bin as before, is given in fig. 4).

A third component ( $N$ ) is therefore introduced in the fits. The obtained relative abundances and  $\chi^2$  values are shown in

tab. 3. Two examples of  $N_{\mu 200}$  distributions in two bins of shower sizes (below and above the knee) are shown in figs. 5 and 6 together with the contributions of each single component. The description of the data is now quite satisfactory as can be deduced also from the  $\chi^2$  values.

The relative abundances of the three elements in the six ranges of shower sizes are given in fig. 7.

By using the size to energy conversions for all primaries

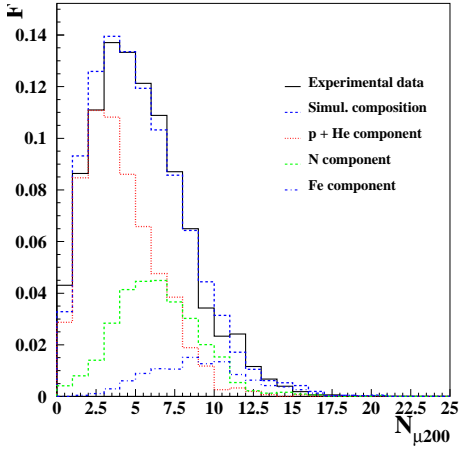


**Fig. 5.**  $N_{\mu 200}$  distribution of the data and expectations with a three component composition in the range  $5.8 < \text{Log}(N_e) < 6.0$ . The contribution of each element is also plotted. ( $N_t = 5206$ )

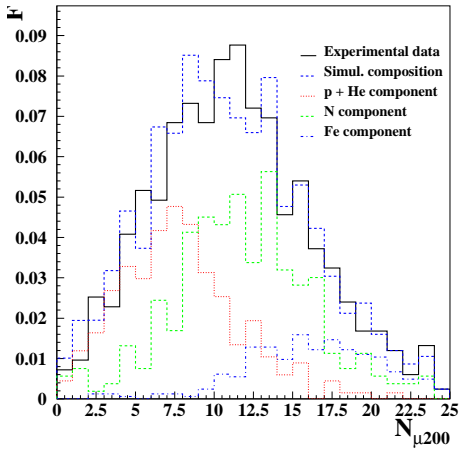


**Fig. 6.** Same as fig. 5, for  $6.2 < \text{Log}(N_e) < 6.4$ . ( $N_t = 907$ )

obtained through the same simulation, and the relative abundances of fig. 7, such abundances can be expressed in terms of primary energy (see fig. 8).

## 5 Conclusions

The analysis of the fluctuations of the muon numbers recorded at core distances  $r_c \approx 200\text{m}$  in narrow intervals of shower sizes is in agreement with an increasing mass of the primaries in the region of the knee. At the lower energies ( $E_0 \approx 10^{15}$  eV) the results reproduce the expectations from the extrapolations of the low energy data (simulations are performed through the CORSIKA/QGSJET code). The mean value  $\langle \ln A \rangle$  deduced from the present analysis, with the three components ("light" + N + Fe) fit, ranges from  $\approx 1.5$  at  $E_0 = 2 \cdot 10^{15}$  to  $\approx 2.4$  at  $E_0 = 8 \cdot 10^{15}$  eV (with statistical errors  $\approx 0.1$ ). The conclusion is consistent with

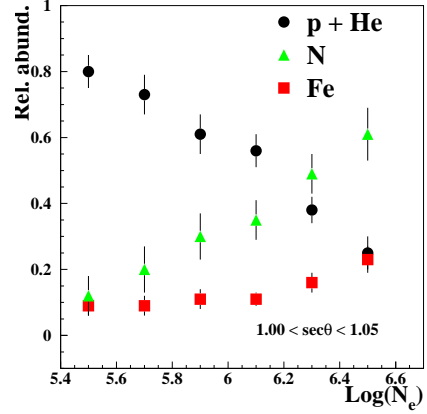


**Fig. 7.** Relative abundances of the three elements in different intervals of shower sizes.

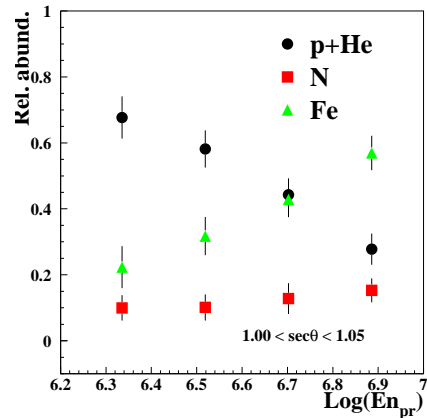


**Fig. 8.** Relative abundances of the three elements as a function of primary energy.

the one reached in an analogous  $N_e$ -muon data analysis by (Kascade Collaboration 1999 b).

While some features of the evolution of the primary composition can depend on some technical choices in the analysis, the main result, of a knee due to the bending of the spectrum of the "light" component, represents anyway a stable solution.

## References

- Aglietta M. et al., Nucl. Inst. Meth. Phys. Res., A 336, p.310, 1993
- The Eas-Top Collaboration, Proc. 25th ICRC, Vol. 4, p.13, 1997
- Chiavassa A. et al, Proc. 26th ICRC, Vol. 1, p.230, 1999
- Forschungszentrum Karlsruhe Report FZKA 6019, 1998
- Kamata K. et al., Suppl. Prog. Theo. Phys., 6, p.93, 1958
- The Kascade Collaboration, Proc. 26th ICRC, Vol.1, p.131, 1999
- The Eas-Top Collaboration, These Proc., 2001
- The Kascade Collaboration, Proc. 26th ICRC, HE 2.2.42, 1999